Inorganic Chemistry

Article

pubs.acs.org/IC

Dy(III) Single-Ion Magnet Showing Extreme Sensitivity to (De)hydration

Min Ren,[†,‡] Dawid Pinkowicz,*[,†,§] Minyoung Yoon,[∥] Kimoon Kim,[∥] Li-Min Zheng,[‡] Brian K. Breedlove,[†] and Masahiro Yamashita*[,†]

[†]Department of Chemistry, Graduate School of Science, Tohoku University, 6-3 Aramaki-Aza-Aoba, Aobaku, Sendai 980-8578, Japan

[‡]State Key Laboratory of Coordination Chemistry, School of Chemistry and Chemical Engineering, Nanjing University, Nanjing 210093, China

[§]Faculty of Chemistry, Jagiellonian University, Ingardena 3, 30-060 Kraków, Poland

[∥]Center for Self-assembly and Complexity, Institute for Basic Science and Center for Smart Supramolecules, Department of Chemistry, Division of Advanced Materials Science, Pohang University of Science and Technology, San 31, Hyojadong, Pohang, 790-784, Republic of Korea

Supporting Information

ABSTRACT: A new mononuclear dysprosium(III)-cucurbit[6]uril complex has been synthesized and characterized structurally and magnetically. It exhibits single-ion magnet (SIM) behavior with two slow magnetic relaxation processes, which are very sensitive to the solvation degree of the sample. Depending on the amount and type of the solvent in the structure, it is possible to switch the slow magnetic relaxation of this compound between the temperature-independent and temperature-dependent regimes.

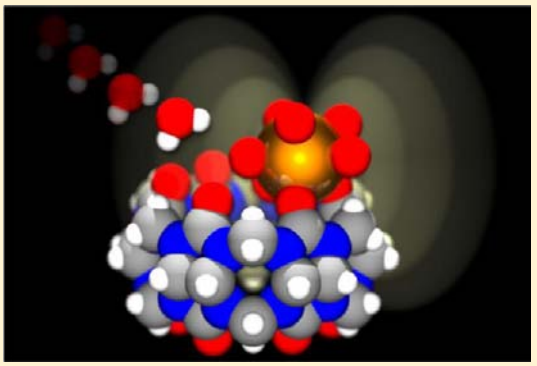

INTRODUCTION

It is widely believed that single-molecule magnets (SMMs) will be the key building blocks in the construction of ultrahigh-density memory components and quantum computing or spintronic devices.[1−3] Recently, SIMs that exhibit slow magnetic relaxation of a single-ion origin attract interest due to their significant magnetic anisotropy, high energy barriers, high blocking temperatures,[4−13] and complex relaxation behavior.[12,14−17] The mechanisms for the reversal of the magnetic moment may involve only the ground state (direct relaxation) or the ground state and some excited states (Orbach and Raman relaxation).[18−20] The direct relaxation process, such as quantum tunneling of the magnetization (QTM), is temperature independent, whereas the other pathways are thermal pathways. Both relaxation processes are observed in SIMs, leading to their complex magnetic behavior.[16b]

It is also well-known that molecular magnets are very sensitive to various external stimuli (e.g., solvent, light, pressure), and SIMs are the same. It has been shown that the relaxation of the magnetization of a lanthanide-based SIM is very sensitive to the coordination environment of the metal center[12,14−17] However, the influence of the crystallization solvent on the magnetic relaxation of SIMs has not been studied in a systematic way. With this in mind, we synthesized a new dysprosium-based SIM $[Dy\{CB[6](NO_3)(H_2O)_4\}](NO_3)_2\cdot 8H_2O$ **1** and investigated its magnetic properties with respect to the "solvation" degree (CB[6] = cucurbit[6]uril, $C_{36}H_{36}N_{24}O_{12}$).[21,22] **1** exhibited multiple magnetic relaxation processes, including a secondary temperature-independent slow relaxation. The SIM behavior of **1** was also found to be sensitive to its "(de)hydration" degree and "(de)hydration history". Therefore, the magnetic properties of **1** were investigated in three different states: **1·initial**, sample transferred directly from the mother liquor to pure water (measured in water); **1·dry**, separated by filtration, washed with MeOH, and dried (measured as dry powder); and **1·water**, separated by filtration, treated with MeOH, dried, and then immersed in water (measured in water).

EXPERIMENTAL SECTION

General Considerations. Chemicals and solvents used in the following syntheses were of reagent grade and were used without further purification (obtained from Aldrich, Tokyo Chemical Industry, or Wako Chemicals GmbH). Methanol (MeOH) was of super-dehydrated grade. The ligand cucurbit[6]uril (CB[6]; $C_{36}H_{36}N_{24}O_{12}$) was prepared according to literature procedures.[23] The synthesis of compound **1** refers to the previously reported one for other

Received: November 18, 2012
Published: July 23, 2013

   dx.doi.org/10.1021/ic400430q | Inorg. Chem. 2013, 52, 8342−8348

lanthanides.[24] All operations were carried out under aerobic conditions.

Preparation of 1 and 1·initial [Dy{CB[6](NO$_3$)(H$_2$O)$_4$}](NO$_3$)$_2$·8H$_2$O. Compound **1** was obtained from a solution containing Dy(III) nitrate and cucurbit[6]uril. A suspension of CB[6] (0.04 mmol, 41 mg) and a large excess of Dy(NO$_3$)$_3$·5H$_2$O (1 mmol, 460 mg) in water (5 mL) was prepared and heated for 10 min on a hot plate with stirring. The resulting solution was filtered while hot. Colorless crystals of compound **1** were obtained after 4 days. They were separated from the mother liquor by decantation using pure water and stored in water as **1·initial**. Yield: 32 mg (52% based on CB[6]). Elemental analysis of **1·initial** is consistent with the formula [Dy{CB[6](NO$_3$)(H$_2$O)$_4$}](NO$_3$)$_2$·8H$_2$O determined from single-crystal X-ray (scXRD) diffraction experiment. Anal. Calcd for C$_{36}$H$_{60}$N$_{27}$O$_{33}$Dy: C, 27.69; H, 3.87; N, 24.22. Found: C, 27.76; H, 3.64; N, 24.06. Selected IR (KBr pellet, cm^{-1}): 3360(br), 3014(w), 2946(w), 1728(s), 1487(s), 1418(w), 1384(m), 1328(m), 1297(w), 1258(w), 1236(m), 1193(m),1149(m), 967(s), 820(w), 802(m), 760(m), 678(m), 634(m).

Preparation of 1·dry [Dy{CB[6](NO$_3$)(H$_2$O)$_4$}](NO$_3$)$_2$·6H$_2$O·MeOH. Crystals of **1** were separated by filtration from the mother liquor, washed with a small amount of water followed by MeOH, and dried in air. Anal. Calcd for C$_{37}$H$_{60}$N$_{27}$O$_{32}$Dy: C, 28.53; H, 3.88; N, 24.28. Found: C, 28.36; H, 3.93; N, 24.11.

Preparation of 1·water [Dy{CB[6](NO$_3$)(H$_2$O)$_4$}](NO$_3$)$_2$·7H$_2$O. Crystals of **1** were separated by filtration from the mother liquor, washed with a small amount of water followed by MeOH, dried in air, immersed in H$_2$O, and then stored in H$_2$O. Anal. Calcd for C$_{36}$H$_{58}$N$_{27}$O$_{32}$Dy: C, 28.01; H, 3.79; N, 24.50. Found: C, 28.01; H, 3.77; N, 24.13.

Physical Measurements. Infrared spectra were collected on JASCO FT/IR-620 Fourier transform spectrometer in KBr pellets. Powder X-ray (PXRD) diffraction experiments were performed using a Rigaku RINT-2500HK diffractometer with Cu Kα radiation (λ = 1.5418 Å) at room temperature in the 3−50° range with 0.02° step for freshly prepared well-ground samples loaded into a narrow diameter borosilicate-glass tube (0.5 mm in diameter; Hilgenberg). Samples **1·initial** and **1·water** were loaded in the form of a suspension in H$_2$O and measured in H$_2$O. Elemental analyses were performed immediately after removing the samples from the appropriate solvent followed by very short drying.

Single-Crystal X-ray Diffraction. Crystallographic data were collected at T = 269(1) K on a Bruker Apex II CCD diffractometer with graphite monochromated Mo Kα radiation (λ = 0.71073 Å) using a crystal mounted in a sealed borosilicate tube (0.3 mm in diameter; Hilgenberg) with a droplet of mother solution beneath it. Data processing was accomplished with the SAINT processing program.[25] The structure was solved by direct methods using SIR-97.[26] Refinement and further calculations were carried out using SHELXL-97.[27] The non-H atoms were refined anisotropically using weighted full-matrix least-squares on F^2. Hydrogen atoms joined to C atoms of CB[6] ligand were positioned with an idealized geometry and refined using riding model. Hydrogen atoms joined to oxygen atoms of crystallization and coordination water could not be found from the difference Fourier map. Crystallographic data for **1·initial**: C$_{36}$H$_{36}$N$_{27}$O$_{33}$Dy, M_r = 1537.42; crystal system, orthorhombic; space group, *Pna*2$_1$; a = 32.006(8) Å, b = 14.851(4) Å, c = 11.859(3) Å, V = 5637(2) Å^3, Z = 4, D_c = 1.812 g cm^{-3}, R_{int} = 0.0404, 60 454 reflections collected, R_1 (wR_2) = 0.0499 (0.1279) and S = 1.100 for 12 986 observed reflections out of 15 601 unique reflections with $I > 2\sigma(I)$.

Magnetic Measurements. Magnetic measurements were performed using Quantum Design MPMS-5S and Quantum Design MPMS SQUID VSM magnetometers. Samples **1·initial** and **1·water** together with a small amount of deionized water (ca. 100 μL) were loaded into a borosilicate glass tubes (60 mm long, 5 mm in diameter, and with 1.0 mm thick walls) and sealed with a torch. This tube together with another empty one were fixed in a drinking straw (Figure S1 in the Supporting Information). Because of the length of the tubes, they are permanently present in all detecting coils of the SQUID magnetometer, and hence they practically do not contribute to the overall magnetization of the studied samples. Sample **1·dry** was measured in a gel capsule using *n*-eicosan to restrain the crystallites from moving. The magnetic data were corrected for the diamagnetic contributions of the sample holders, immersion water or *n*-eicosan, and diamagnetism of the samples themselves using Pascal constants.[28]

RESULTS AND DISCUSSION

Structural Analysis. Compound **1** crystallized in the orthorhombic space group *Pna*2$_1$. Selected crystallographic data are summarized in the Experimental Section, and the crystal structure of **1** is shown in Figure 1 and Figure S2 in the

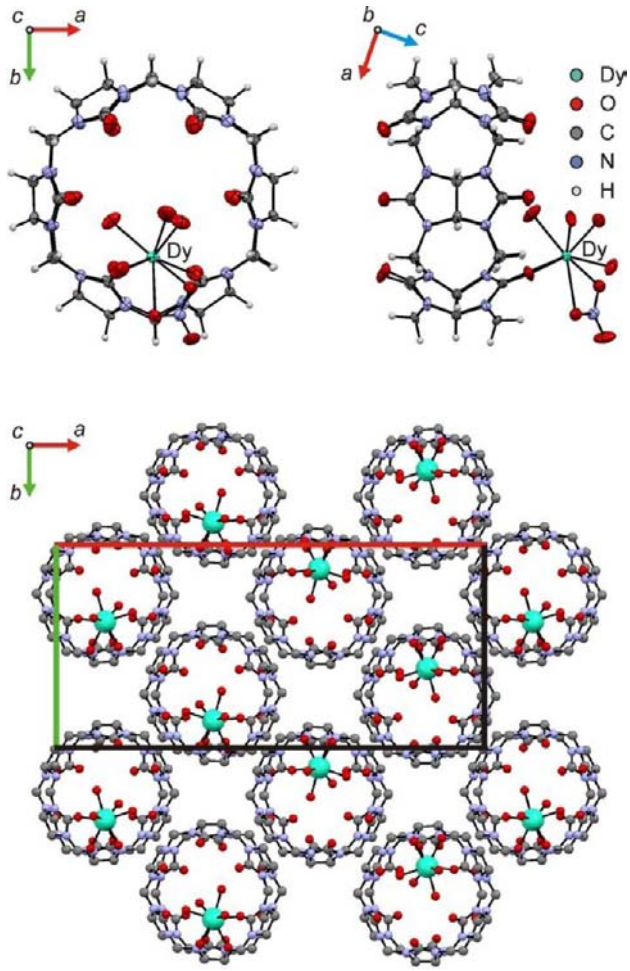

Figure 1. Top and side views of the molecular structure of **1** (top) and its packing diagram (bottom: crystallization water, nitrate anions, and hydrogen atoms omitted for clarity).

Supporting Information. The asymmetric unit (Figure S2) consists of one Dy(III) ion, one CB[6] molecule, three NO$_3^-$ counteranions, and 12 water molecules. Each Dy(III) ion is eight coordinated by two carbonyl oxygen atoms of CB[6], two oxygen atoms of a nitrate anion in a bidentate mode, and the remaining coordination sites are filled with four *aqua* ligands. The Dy(III) ion is coordinated to one of the portals of CB[6] and leans toward its side. Table S1 (Supporting Information) presents the bond lengths of the [DyO$_8$]-core. The coordination geometry of the Dy-center is severely distorted due to the bidentate coordination mode of the nitrate ligand. From Continuous Shape Measure (CShM) analysis of the Dy coordination sphere, its geometry cannot be described as a dodecahedron, a bicapped trigonal prism, or a square antiprism.

dx.doi.org/10.1021/ic400430q | Inorg. Chem. 2013, 52, 8342−8348

The obtained values of CShM deviate significantly from zero for all three ideal shapes (Table S2 in the Supporting Information).[29] In addition, the Δ values describing the deviation from the interconversion pathways between these three limiting geometries are much larger than 0.1, indicating significant distortion from the ideal shapes.[30]

All Dy-CB[6] units are "stacked" along the crystallographic *c*-axis in a way depicted in Figure 1 (bottom), forming channels filled with crystallization water. The units are connected with each other through the network of hydrogen bonds involving carbonyl groups of CB[6], nitrate anions, and coordination and crystallization water molecules (Figure 2). The hydrogen-bond

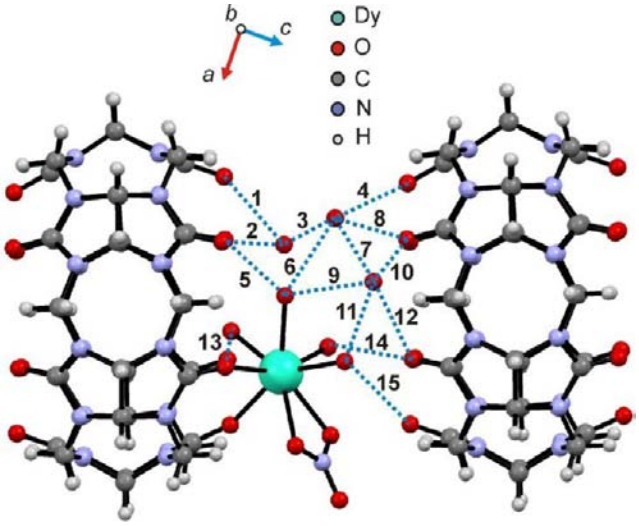

Figure 2. Hydrogen bonding in **1** between crystallization water, coordination water, and the two adjacent CB[6] molecules with donor–acceptor distances: (1) 2.718 Å, (2) 2.817 Å, (3) 2.704 Å, (4) 2.926 Å, (5) 2.569 Å, (6) 2.753 Å, (7) 2.593 Å, (8) 2.593 Å, (9) 3.194 Å, (10) 2.762 Å, (11) 2.715 Å, (12) 3.345 Å, (13) 2.779 Å, (14) 2.635 Å, (15) 2.691 Å.

network stabilizes effectively the supramolecular channeled structure of **1** as long as its sample is stored in water. However, when taken out of the mother liquor, the crystals of **1** lose crystallization water easily and fall apart. Because the loss of solvent from molecular magnetic solids can dramatically affect their structural and magnetic properties,[14,15] we investigated this phenomenon more thoroughly. Three different samples of **1** have been prepared showing different content of crystallization solvent (based on elemental analyses; see Experimental Section): $[Dy\{CB[6](NO_3)(H_2O)_4\}](NO_3)_2{\cdot}8H_2O$ **1·initial** (equivalent to **1**) with eight crystallization H_2O's; $[Dy\{CB[6](NO_3)(H_2O)_4\}](NO_3)_2{\cdot}6H_2O{\cdot}MeOH$ **1·dry** with six crystallization H_2O's plus one MeOH molecule; and $[Dy\{CB[6](NO_3)(H_2O)_4\}](NO_3)_2{\cdot}7H_2O$ **1·water** with only seven crystallization H_2O's. Structural scXRD study of these three different crystal phases was not possible because the crystals of **1** were falling apart upon drying. Powder XRD experiments did not show any obvious structural changes. All PXRD patterns, the one simulated from the scXRD data and the experimental ones of **1·initial**, **1·dry**, and **1·water**, look the same (Figure 3).

Magnetic Properties. The thermal (T) dependence of the molar magnetic susceptibility (χ_M) of all three samples was measured in an applied direct current (DC) field of H = 1000 Oe in the temperature range of 1.8–300 K. Figure 4 shows $\chi_M T$

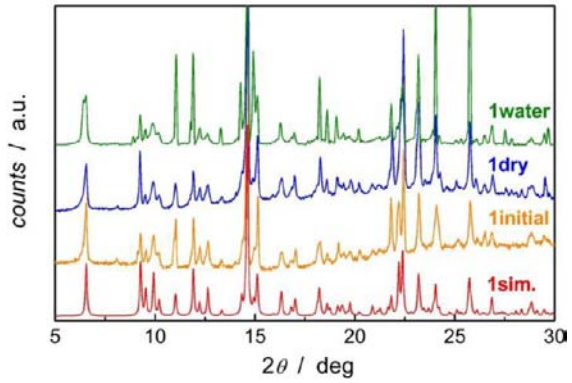

Figure 3. Experimental and simulated PXRD patterns of compound **1** in its three different states.

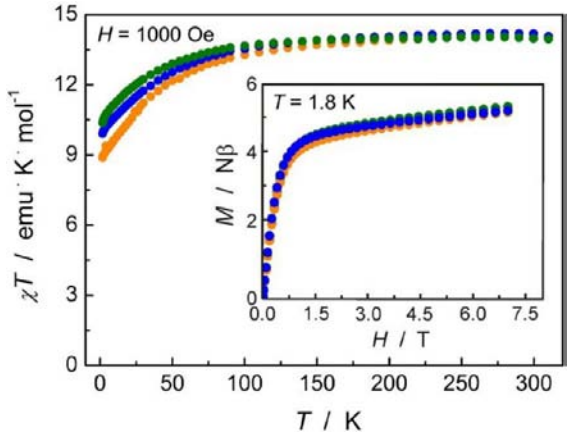

Figure 4. The $\chi_m T$ versus T plots (main) and M versus H plots for **1·initial** (orange), **1·dry** (blue), and **1·water** (olive); solid lines are only guides for the eye.

versus T plots for all three samples. At room temperature, the $\chi_M T$ values were 14.08 (**1·initial**), 14.11 (**1·dry**), and 13.98 (**1·water**) cm^3 K mol^{-1}. These values are in good agreement with the expected value of 14.17 cm^3 K mol^{-1} ($^6H_{15/2}$, S = 5/2, L = 5, g = 4/3). The magnetic susceptibility data in the temperature range of 300–100 K were fitted with the Curie–Weiss law. For each sample, a different Weiss constant (θ) was obtained: −8.74 K (**1·initial**), −6.11 K (**1·dry**), and −7.59 K (**1·water**). The negative values of θ for mononuclear lanthanide complexes are due to their large unquenched orbital momenta. The decrease in the $\chi_M T$ values upon cooling indicates the thermal depopulation of the m_J sublevels and the presence of significant magnetic anisotropy of Dy(III). The magnetization (M) versus field (H) data at 1.8 K for all three samples show a similar rapid increase in the magnetization at low fields (Figure 4, inset). At higher fields above 1 T, the magnetization increases linearly, reaching the values 5.20 Nβ (**1·initial**), 5.24 Nβ (**1·dry**), and 5.35 Nβ (**1·water**) without clear saturation. The observed magnetization at the highest field is much lower than the expected 10 Nβ for Dy(III) ion, which together with the nonsuperposition of the M versus $H{\cdot}T^{-1}$ curves recorded at different temperatures (Figure S3 in the Supporting Information) suggest the presence of a large magnetic anisotropy in the reported compounds.

Alternating current (AC) magnetic measurements were performed on **1** in the three states in the temperature range of 1.8–10 K (H_{AC} = 3 Oe). In the absence of a DC field, all

dx.doi.org/10.1021/ic400430q | Inorg. Chem. 2013, 52, 8342–8348

three samples of **1** exhibited very weak signals of the out-of-phase magnetic susceptibility, and only a "tail" indicating frequency dependence was observed (Figure S4 in the Supporting Information). Clear frequency-dependent peaks could be observed by applying static DC field (Figure 5). H_{dc} =

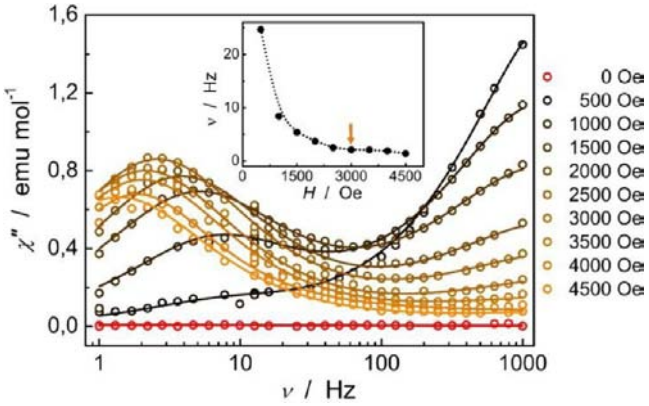

Figure 5. Magnetic field dependence of the in-phase and out-of-phase AC magnetic susceptibility for **1·initial** (main; H_{AC} = 3 Oe; T = 1.8 K Oe) and frequency of the χ'' maximum versus magnetic field plot (inset).

3000 Oe has been found to be the optimum field for **1·initial** determined from the χ'' maximum versus field plot (Figure 5, inset). This dependence does not show a clear minimum, but a plateau, which begins at 3000 Oe. The temperature dependence of the in-phase and out-of-phase AC magnetic susceptibility χ' and χ'' measured in an external DC field of 3000 Oe is shown in Figure S5 in the Supporting Information. The χ'' versus ν dependence of **1·initial** showed two maxima (Figure 6),

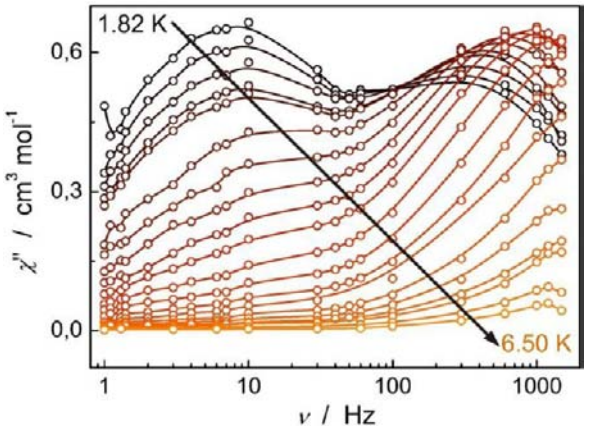

Figure 6. Frequency dependence of the out-of-phase AC magnetic susceptibility for **1·initial** at various temperatures (from 1.82 to 6.50 K; H_{AC} = 3 Oe; H_{DC} = 3000 Oe; solid lines are only guides for the eye).

indicating slow magnetic relaxation. The two peaks suggest that there are two independent magnetic relaxation processes. The similar set of AC measurements for **1·dry** showed only weak frequency dependence with a "half-shaped" maximum in the high frequency region (around 1000 Hz) and a shoulder in the low frequency region (Figure 7). Finally, **1·water** exhibited one well-shaped maximum in the low frequency range (1−50 Hz) and a "tail" in the high frequency region (50−1500 Hz; Figure 8). Cole−Cole plots (χ'' vs χ')[31] also showed the differences

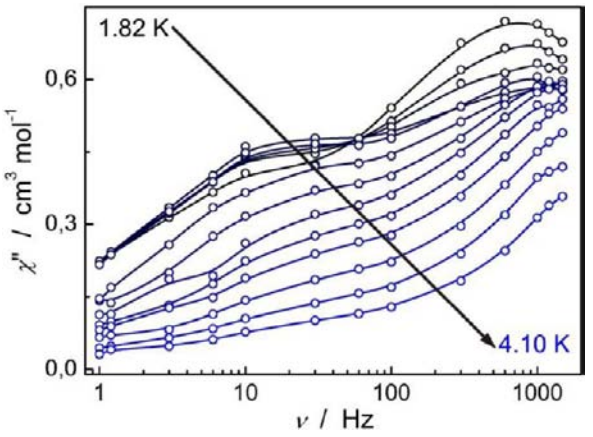

Figure 7. Frequency dependence of the out-of-phase AC magnetic susceptibility for **1·dry** at various temperatures (from 1.82 to 4.10 K; H_{AC} = 3 Oe; H_{DC} = 3000 Oe; solid lines are only guides for the eye).

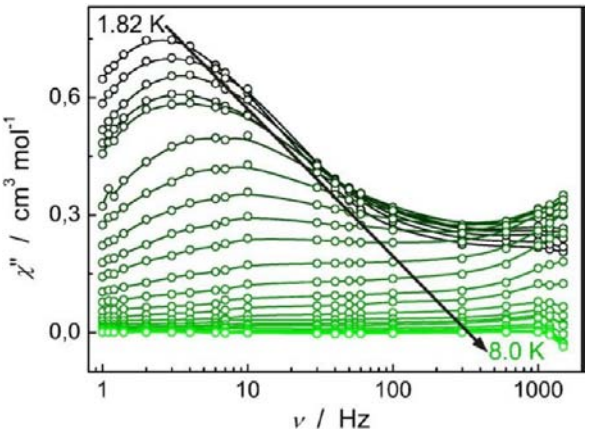

Figure 8. Frequency dependence of the out-of-phase AC magnetic susceptibility for **1·water** at various temperatures (from 1.82 to 8.0 K; H_{AC} = 3 Oe; H_{DC} = 3000 Oe; solid lines are only guides for the eye).

among the three samples of **1**. The magnetic relaxation times τ and α factors, which account for the distribution in the relaxation processes, were obtained by fitting the Cole−Cole plots using the generalized Debye model in eq 1[2] (single relaxation model) and/or a linear combination of two modified Debye models, as shown in eq 2[32] (double relaxation):

$$\chi(\omega) = \chi_S + \frac{\chi_T - \chi_S}{1 + (i\omega\tau)^{1-\alpha}} \quad (1)$$

$$\chi(\omega) = \chi_S + (\chi_T - \chi_S)\left(\frac{f_A}{1 + (i\omega\tau_A)^{1-\alpha_A}} + \frac{1 - f_A}{1 + (i\omega\tau_B)^{1-\alpha_B}}\right) \quad (2)$$

Table 1 summarizes the results obtained from fitting the Cole−Cole plots for all three samples. For **1·initial**, in the temperature range of 1.82−3.8 K, the Cole−Cole plots were fitted using eq 2. Above 3.8 K, only one relaxation was observed (relaxation path A; 50−1500 Hz), and the data were fitted using eq 1 (Figure 9). Relaxation path A was thermally activated above 4.4 K and became temperature independent at low temperature. Such behavior indicates a crossover from an Orbach mechanism to a direct tunneling process.[19,20] The

dx.doi.org/10.1021/ic400430q | Inorg. Chem. 2013, 52, 8342−8348

Table 1. Selected Parameters Obtained by Fitting Cole–Cole Plots of 1·initial, 1·dry, and 1·water with the Debye Model

T/K	state	τ_A/ms	α_A	τ_B/ms	α_B	f_B
1.82	**1·initial**	0.363	0.271	28.6	0.303	0.584
	1·dry	0.201	0.323	22.2	0.418	0.345
	1·water	0.0830	0.453	60.4	0.333	0.763
1.92	**1·initial**	0.347	0.296	27.8	0.288	0.525
	1·dry	0.164	0.326	16.3	0.413	0.400
	1·water	0.0669	0.437	51.4	0.358	0.756
2.40	**1·initial**	0.244	0.280	18.7	0.301	0.384
	1·dry	0.095	0.356	9.47	0.387	0.386
	1·water	0.0477	0.422	26.7	0.372	0.614
2.80	**1·initial**	0.192	0.289	20.1	0.289	0.255
	1·dry	0.0649	0.345	6.54	0.430	0.328
	1·water	0.0276	0.344	17.5	0.456	0.548
3.20	**1·initial**	0.146	0.275	19.3	0.283	0.174
	1·dry	0.0430	0.329	5.63	0.427	0.269
	1·water	0.0201	0.220	10.4	0.524	0.476
3.80	**1·initial**	0.0837	0.263	23.5	0.334	0.105
	1·dry	0.0237	0.336	6.61	0.409	0.154
	1·water	0.0141	0.0427	4.34	0.621	0.375

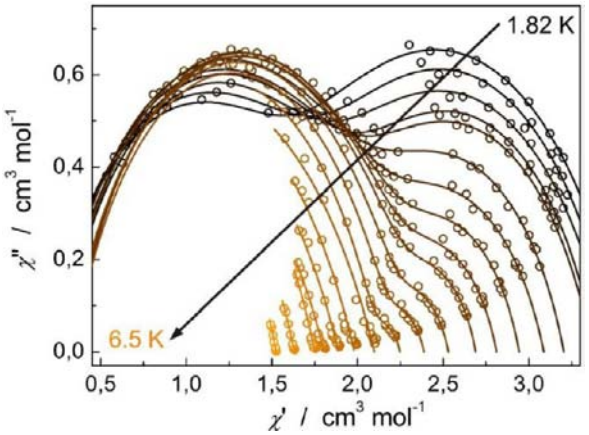

Figure 9. The Cole–Cole plot for **1·initial**. The solid lines represent the best fit to the Debye model eq 2 or eq 1.

anisotropic energy barrier U_{eff} was obtained by fitting the high temperature regime (>4.4 K) to the Arrhenius law $\tau = \tau_0 \exp(U_{eff}/kT)$ (τ-relaxation time). U_{eff} and τ_0 were determined to be 38.4 K and 4.78×10^{-9} s, respectively (Figure 12, orange ▲). The second slow relaxation process (relaxation path B, 1–50 Hz) was temperature independent similar to the QTM behavior observed at low temperature for path A. The average relaxation time for path B below 3.8 K was determined to be 23 ms, which is 2 orders of magnitude slower than that for path A. To the best of our knowledge, such a secondary temperature-independent slow relaxation process is quite rare for molecule-based magnets.[11,13,33] The weight ratio ($f_B = 1 - f_A$) of relaxation path B for **1·initial** decreased from 0.584 to 0.074 upon warming and disappeared above 3.8 K. In the high-temperature regime, relaxation path A became dominant. It is important to mention that relaxation path B was observed in stronger applied magnetic fields. The Cole–Cole plot for **1·dry** is quite different from that of **1·initial** (Figure 10). The weight ratio of relaxation A (f_A) is larger and the relaxation time of A is smaller. In the high temperature region (>4.1 K), the signal of the imaginary component of the AC magnetic susceptibility was

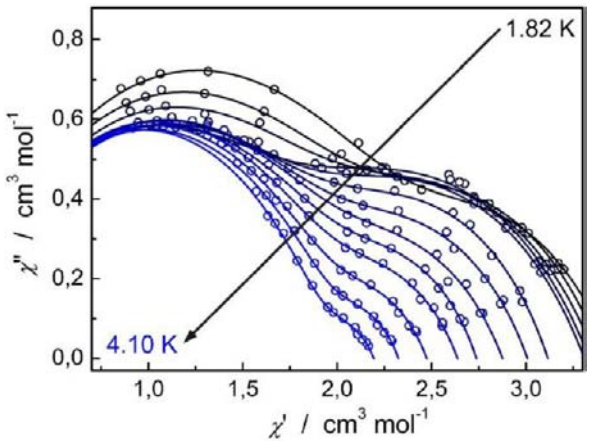

Figure 10. The Cole–Cole plot for **1·dry**. The solid lines represent the best fit to the Debye model eq 2 or eq 1.

too weak to be reliably fitted using the Debye model, and therefore, in the case of **1·dry**, it was not possible to calculate the energy barrier for the relaxation path A. Relaxation path B was temperature independent with an average relaxation time of 8.9 ms (Figure 12, blue symbols). For **1·water**, the Cole–Cole plot was different from that of the two previous ones (Figure 11). Below 3.0 K, relaxation path B was the dominant

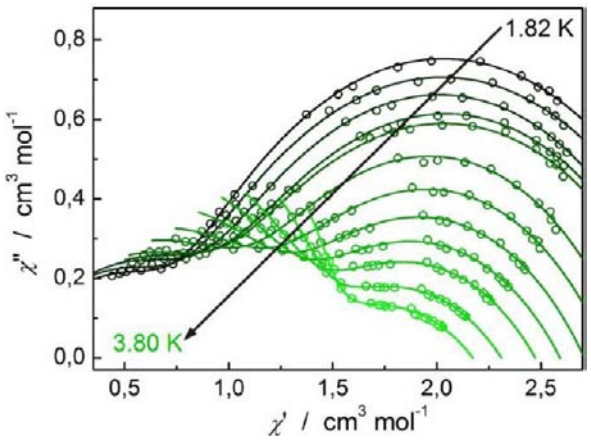

Figure 11. The Cole–Cole plot for **1·water**. The solid lines represent the best fit to the Debye model eq 2 or eq 1.

relaxation pathway, and f_B decreased from 0.763 to 0.519 upon warming. The average relaxation time was determined to be ~22 ms. The out of phase signal in the high temperature region was also very weak, similar to that of **1·dry**, and therefore it could not be fitted (Figure 12, green symbols). Figure 13 shows simulated Cole–Cole curves at 1.82 K for the three samples of **1**. For **1·dry**, relaxation path A was the dominant relaxation process, whereas for **1·water**, B was the main pathway. For **1·initial**, both relaxation pathways A and B were important.

Recently, Long and co-workers have reported a uranium(III)-based single-ion magnet $U(H_2Bpz_2)_3$, which exhibits a field-introduced secondary slow relaxation process[33] similar to the behavior of **1·initial**. Similar behavior was also reported by Car et al. for the Dy^{III}(DOTA) complex.[34]

The different magnetization relaxation behaviors of **1·initial**, **1·dry**, and **1·water** can be attributed to the loss/gain of the crystallization solvent, which probably induces significant structural rearrangement in the compound. Unfortunately,

dx.doi.org/10.1021/ic400430q | Inorg. Chem. 2013, 52, 8342–8348

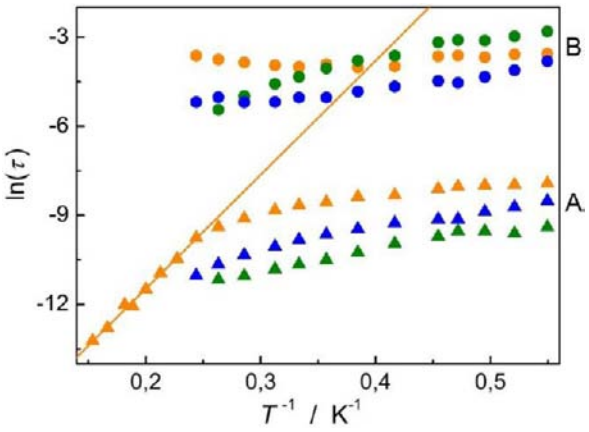

Figure 12. ln(τ) versus T^{-1} plots for relaxation path A (▲) and B (●) in **1·initial** (orange), **1·dry** (blue), and **1·water** (olive). Solid line represents the best fit to the Arrhenius law.

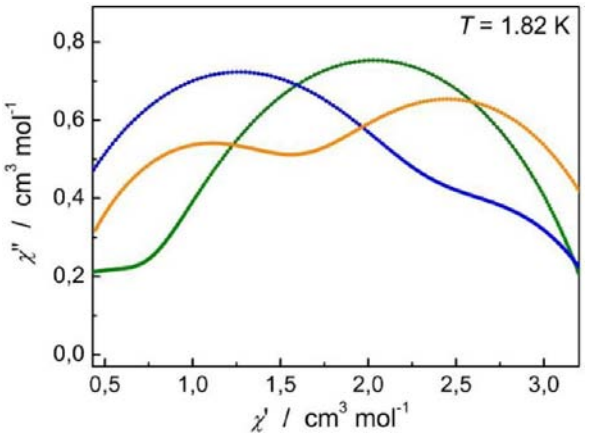

Figure 13. The comparison of the best fits of the Cole–Cole plots using the Debye model for **1·initial** (orange), **1·dry** (blue), and **1·water** (olive) at 1.82 K.

these possible structural changes upon solvent loss could not be followed using single-crystal XRD experiment (the crystals of **1** crack upon drying/solvent exchange). Only PXRD patterns of the three samples were recoded, and there were no obvious differences among them. Experimental PXRD patterns (Figure 3) agree very well with that simulated from single-crystal data. The structural differences induced by solvent exchange are very subtle but still affect the magnetic behavior of **1**. In recent reports, it has been suggested that a change in the orientation of even one water molecule or a change in the location of the hydrogen atoms can play an important role in the orientation of the magnetization easy axis of lanthanide ions.[35,36] In the present study, the loss of crystallization solvent and the possible subsequent changes in the hydrogen-bond network must contribute to the ligand field of Dy(III) ion and its single-ion anisotropy, causing very different magnetic relaxation behaviors. The secondary relaxation process may be also induced/controlled by weak intermolecular interactions pathways provided by the hydrogen bonds. Cleavage of these bonds upon dehydration could also explain the observed sensitivity to crystallization solvent loss/gain and the presence of the secondary relaxation process. Multiple relaxation processes can be induced by intermolecular interactions as it has been shown by Katoh et al. for multiple-decker phthalocyanine complexes of Dy(III) and Tb(III).[16a] Another example is the mononuclear dysprosium compound [Dy(hfac)$_3$(L)] (L = 4,5-bis(propylthio)tetrathiafulvalene-2-(2-pyridyl)-3-(2-pyridylmethyl)benzimidazole) that exhibits two relaxation processes in powder state and only one relaxation in magnetic dilution and frozen solution.[37] Similar to compound [Dy(hfac)$_3$(L)], the dual relaxation processes of **1** can be observed directly in the solid state.

To establish whether the change from **1·dry** to **1·water** is reversible, we have performed a series of basic magnetic measurements on the sample of **1·water** after second drying (referred to as **1·dryII**). At room temperature, the $\chi_M T$ value for **1·dryII** was 14.19 cm^3 K mol^{-1} very close to 14.11 cm^3 K mol^{-1} (**1·dry**). The $\chi_M T$ versus T plots at H_{DC} = 1000 Oe have identical shape for both samples (Figure S6, top in the Supporting Information). The M versus H plots at 1.8 K are also identical. The Cole–Cole plot for **1·dryII** recorded at 2.0 K shows that the fast relaxation path A is the dominant one, similar to **1·dry** (Figure S6, bottom in the Supporting Information). All of this suggests that the transformation between **1·dry** and **1·water** is reversible.

CONCLUSIONS

Unlike most SIMs, [Dy{CB[6](NO$_3$)(H$_2$O)$_4$}](NO$_3$)$_2$·8H$_2$O **1** exhibited two slow magnetic relaxation processes. Additionally, its magnetic relaxation behavior and particularly the weight ratio of the dual relaxation processes are very sensitive to the structural changes induced by the loss/gain of the solvent of crystallization. This unique feature allows for reversible switching between the two slow magnetic relaxation pathways in **1** by controlling the solvation degree of the sample. This interesting behavior was only uncovered because we performed additional magnetic measurements on our compound prepared in three different ways. Our study clearly shows that placing the sample under vacuum in the magnetometer's sample chamber can seriously affect the magnetic data. Currently, we are further studying the magnetic behavior of **1**, including measurements on a magnetically diluted samples. We are also planning detailed calculations to fully explain the mechanism of the magnetic relaxations in this compound.

ASSOCIATED CONTENT

Supporting Information

Additional magnetic data, figures, and tables with XRD data. This material is available free of charge via the Internet at http://pubs.acs.org.

AUTHOR INFORMATION

Corresponding Author

*Phone: +81-22-795-6544. Fax: +81-22-795-6548. E-mail: pinkowic@chemia.uj.edu.pl (D.P.); yamasita@agnus.chem.tohoku.ac.jp (M.Y.).

Notes

The authors declare no competing financial interest.

ACKNOWLEDGMENTS

This work was financially supported by a Grant-in-Aid for Scientific Research (S) (grant no. 20225003). D.P. gratefully acknowledges the financial support of the Matsumae International Foundation within the 2012 Fellowship Programme and the support of the Foundation for Polish Science within the START Programme. K.K. gratefully acknowledges the Research

Center Program (Project No. CA1203) of the Institute for Basic Science (IBS) and World Class University (Project No. R31-2008-000-10059-0) in Korea.

REFERENCES

(1) Gatteschi, D.; Sessoli, R. *Angew. Chem., Int. Ed.* **2003**, *42*, 268.
(2) Gatteschi, D.; Sessoli, R.; Villain, J. *Molecular Nanomagnets*; Oxford University Press: New York, 2006.
(3) Bogani, L.; Wernsdorfer, W. *Nat. Mater.* **2008**, *7*, 179.
(4) Rinehart, J. D.; Long, J. R. *Chem. Sci.* **2011**, *2*, 2078.
(5) Zadrozny, J. M.; Long, J. R. *J. Am. Chem. Soc.* **2011**, *133*, 20732.
(6) Ishikawa, N.; Sugita, M.; Ishikawa, T.; Koshihara, S.-Y.; Kaizu, Y. *J. Am. Chem. Soc.* **2003**, *125*, 8694.
(7) AlDamen, M. A.; Clemente-Juan, J. M.; Coronado, E.; Martí-Gastaldo, C.; Gaita-Ariño, A. *J. Am. Chem. Soc.* **2008**, *130*, 8874.
(8) Rinehart, J. D.; Long, J. R. *J. Am. Chem. Soc.* **2009**, *131*, 12558.
(9) Freedman, D. E.; Harman, W. H.; Harris, T. D.; Long, G. J.; Chang, C. J.; Long, J. R. *J. Am. Chem. Soc.* **2010**, *132*, 1224.
(10) Jiang, S.-D.; Wang, B.-W.; Su, G.; Wang, Z.-M.; Gao, S. *Angew. Chem., Int. Ed.* **2010**, *49*, 7448.
(11) Jiang, S.-D.; Wang, B.-W.; Sun, H.-L.; Wang, Z.-M.; Gao, S. *J. Am. Chem. Soc.* **2011**, *133*, 4730.
(12) (a) Jeletic, M.; Lin, P.-H.; Le Roy, J. J.; Korobkov, I.; Gorelsky, S. I.; Murugesu, M. *J. Am. Chem. Soc.* **2011**, *133*, 19286. (b) Suzuki, K.; Sato, R.; Mizuno, N. *Chem. Sci.* **2013**, *4*, 596−600. (c) Song, Y.-M.; Luo, F.; Luo, M.-B.; Liao, Z.-W.; Sun, G.-M.; Tian, X.-Z.; Zhu, Y.; Yuan, Z.-J.; Liu, S.-J.; Xu, W.-Y.; Feng, X.-F. *Chem. Commun.* **2012**, *48*, 1006−1008. (d) Ruiz, J.; Mota, A. J.; Rodríguez-Diéguez, A.; Titos, S.; Herrera, J. M.; Ruzi, E.; Cremades, E.; Costes, J. P.; Colacio, E. *Chem. Commun.* **2012**, *48*, 7916−7918. (e) Woodruff, D. N.; Winpenny, R. E. P.; Layfield, R. A. *Chem. Rev.* **2013**, *113*, 5110. (f) Zhang, P.; Guo, Y.-N.; Tang, J. *Coord. Chem. Rev.* **2013**, *257*, 1728−1763.
(13) Magnani, N.; Apostolidis, C.; Morgenstern, A.; Colineau, E.; Griveau, J.-C.; Bolvin, H.; Walter, O.; Caciuffo, R. *Angew. Chem., Int. Ed.* **2011**, *50*, 1696.
(14) Ritchie, C.; Speldrich, M.; Gable, R. W.; Sorace, L.; Kögerler, P.; Boskovic, C. *Inorg. Chem.* **2011**, *50*, 7004.
(15) (a) Murrie, M.; Teat, S. J.; Stoeckli-Evans, H.; Güdel, H. U. *Angew. Chem., Int. Ed.* **2003**, *42*, 4653. (b) Pinkowicz, D.; Podgajny, R.; Gaweł, B.; Nitek, W.; Łasocha, W.; Oszajca, M.; Czapla, M.; Makarewicz, M.; Bałanda, M.; Sieklucka, B. *Angew. Chem., Int. Ed.* **2011**, *50*, 3973.
(16) (a) Katoh, K.; Horii, Y.; Yasuda, N.; Wernsdorfer, W.; Toriumi, K.; Breedlove, B. K.; Yamashita, M. *Dalton Trans.* **2012**, *41*, 13582. (b) Watanabe, A.; Yamashita, A.; Nakano, M.; Yamamura, T.; Kajiwara, T. *Chem.-Eur. J.* **2011**, *17*, 7428. (c) Car, P.-E.; Perfetti, M.; Mannini, M.; Favre, A.; Caneschi, A.; Sessoli, R. *Chem. Commun.* **2011**, *47*, 3751.
(17) Xue, S.; Zhao, L.; Guo, Y.-N.; Chen, X.-H.; Tang, J. *Chem. Commun.* **2012**, *48*, 7031.
(18) Ishikawa, N.; Sugita, M.; Ishikawa, T.; Koshihara, S.-Y.; Kaizu, Y. *J. Phys. Chem. B* **2004**, *108*, 11265.
(19) Abragam, A.; Bleaney, B. *Electron Paramagnetic Resonance of Transition Ions*; Oxford University Press: Clarendon, 1970.
(20) Standley, K. J.; Vaughan, R. A. *Electron Spin Rexalation Phenomena in Solids*; Hilger: London, 1969.
(21) Samsonenko, D. G.; Lipkowski, J.; Gerasko, O. A.; Virovets, A. V.; Sokolov, M. N.; Fedin, V. P.; Platas, J. G.; Hernandez-Molina, R.; Mederos, A. *Eur. J. Inorg. Chem.* **2002**, 2380.
(22) Masson, E.; Ling, X.; Joseph, R.; Kyeremeh-Mensah, L.; Lu, X. *RSC Adv.* **2012**, *2*, 1213.
(23) Freeman, W. A.; Mock, W. L.; Shih, N.-Y. *J. Am. Chem. Soc.* **1981**, *103*, 7367.
(24) Samsonenko, D. G.; Lipkowski, J.; Gerasko, O. A.; Virovets, A. V.; Sokolov, M. N.; Fedin, V. P.; Platas, J. G.; Hernandez-Molina, R.; Mederos, A. *Eur. J. Inorg. Chem.* **2002**, 2380−2388.
(25) Bruker. *SAINT*; Bruker AXS Inc.: Madison, WI, 2007.
(26) Altomare, A.; Burla, M. C.; Camalli, M.; Cascarano, G. L.; Giacovazzo, C.; Guagliardi, A.; Moliterni, A. G. G.; Polidori, G.; Spagna, R. *J. Appl. Crystallogr.* **1999**, *32*, 115.
(27) Sheldrick, G. M. *Acta Crystallogr.* **2008**, *A64*, 112−122.
(28) Olivier, K. *Molecular Magnetism*; VCH Publishers, Inc.: New York, 1993.
(29) Pinsky, M.; Avnir, D. *Inorg. Chem.* **1998**, *37*, 5575.
(30) Casanova, D.; Llunell, M.; Alemany, P.; Alvarez, S. *Chem.-Eur. J.* **2005**, *11*, 1479.
(31) Cole, K. S.; Cole, R. H. *J. Chem. Soc.* **1941**, *9*, 341.
(32) Domingo, N.; Luis, F.; Nakano, M.; Muntó, M.; Gómez, J.; Chaboy, J.; Ventosa, N.; Campo, J.; Veciana, J.; Ruiz-Molina, D. *Phys. Rev. B* **2009**, *79*, 214404.
(33) Rinehart, J. D.; Meihaus, K. R.; Long, J. R. *J. Am. Chem. Soc.* **2010**, *132*, 7572.
(34) Cucinotta, G.; Perfetti, M.; Luzon, J.; Etienne, M.; Car, P.-E.; Caneschi, A.; Calvez, G.; Bernot, K.; Sessoli, R. *Angew. Chem., Int. Ed.* **2012**, *51*, 1606.
(35) Moro, F.; Mills, D. P.; Liddle, S. T.; van Slageren, J. *Angew. Chem., Int. Ed.* **2013**, *52*, 3430.
(36) Murugesu, M. *Nat. Chem.* **2012**, *4*, 347.
(37) Cosquer, G.; Pointillart, F.; Golhen, S.; Cador, O.; Ouahab, L. *Chem.-Eur. J.* **2013**, *19*, 7895.